

On the iron $K\alpha$ complex in magnetic cataclysmic variables

Coel Hellier¹ & Koji Mukai²

¹*School of Chemistry and Physics, Keele University, Staffordshire, ST5 5BG*

²*Laboratory for High Energy Astrophysics, NASA/GSFC, Code 662, Greenbelt, MD 20771, USA*

17 November 2018

ABSTRACT

We present a compilation of spectra of the iron $K\alpha$ region in magnetic cataclysmic variables, using data from the *Chandra*-HETG. The H-like, He-like and fluorescent components are clearly resolved, and there are hints of the structure within each component. The different shape of the He-like component in AM Her might be related to greater cyclotron cooling in this star. A surprising absence of Doppler shifts in the H-like and He-like components implies that the X-ray emission is predominantly from the denser, lower-velocity base of the accretion columns. This absence will allow *Astro-E2* to resolve the structure in each component, leading to temperature diagnostics.

We do not confirm the report that the H-like and He-like components of AO Psc are Compton broadened; however we do detect a Compton-downshifted shoulder to the fluorescent line of GK Per. Further, a Doppler-shifted wing of this line arises in the high-velocity, pre-shock flow.

Key words: accretion, accretion discs – novae, cataclysmic variables – binaries: close – X-rays: stars.

1 INTRODUCTION

The iron $K\alpha$ complex is the strongest emission line in the X-ray spectra of magnetic cataclysmic variables (MCVs). In such stars an accretion shock above the white dwarf surface heats accreting material to ~ 30 keV. The highly ionized, optically thin plasma then cools and settles onto the white dwarf, eventually becoming optically thick. The observed X-ray emission is thus the sum of contributions from a range of temperatures, densities, and optical depths (e.g., Aizu 1973; Cropper et al. 1999).

In principle, the emission lines will provide diagnostics of the accretion flow in MCVs [see Fujimoto & Ishida (1997) for a determination of white dwarf mass, and Mauche, Liedahl & Fournier (2001; 2003) for density diagnostics] though the inhomogeneity of the accretion column complicates the interpretation. The relative contributions of collisional ionization and photo-ionization are also uncertain: Mukai et al. (2003) argue that photo-ionization dominates the spectrum at high mass-accretion rates but not at lower rates.

Early studies of the Fe $K\alpha$ line in MCVs (e.g. Norton, Watson & King 1991) used data that had insufficient resolution to resolve the components from H-like, He-like and colder iron. This was first possible with the CCD detectors on the ASCA satellite, which gave 120-eV resolution. Using ASCA data, Hellier, Mukai & Osborne (1998) claimed that in some MCVs (e.g. V1223 Sgr) the three components were clearly resolved, whereas in others (e.g. AO Psc) the

components appeared broadened and blended. The ~ 150 -eV broadening was attributed to Compton scattering.

The high-energy transmission grating (HETG) on *Chandra* is a further advance: though it has a lower effective area than the ASCA CCDs, its 35-eV resolution is sufficient to separate the three main components with ease, and to discern some of the structure within the components. The forthcoming *Astro-E2* will be better still, with 6-eV resolution and a high effective area. In this paper we report the appearance of the Fe $K\alpha$ complex at the *Chandra*-HETG resolution, based on a compilation of MCV spectra.

2 OBSERVATIONS AND RESULTS

Five MCVs have so far been observed with the *Chandra*-HETG, namely AO Psc, AM Her, EX Hya, V1223 Sgr and GK Per. The observations are listed in Table 1. For each we extracted the HEG (high energy) and MEG (medium energy) spectra, combining the +1 and –1 orders.

The GK Per data consist of two observations taken during the 2002 outburst when the optical magnitudes were 11.0 and 10.5. In our analysis we have summed the two spectra. The AM Her spectra were obtained in an intermediate brightness state at an optical magnitude of 14; the AO Psc, V1223 Sgr and EX Hya spectra were obtained in the usual state of these stars.

Fig. 1 shows the iron $K\alpha$ region of HEG data for each

arXiv:astro-ph/0405254v1 13 May 2004

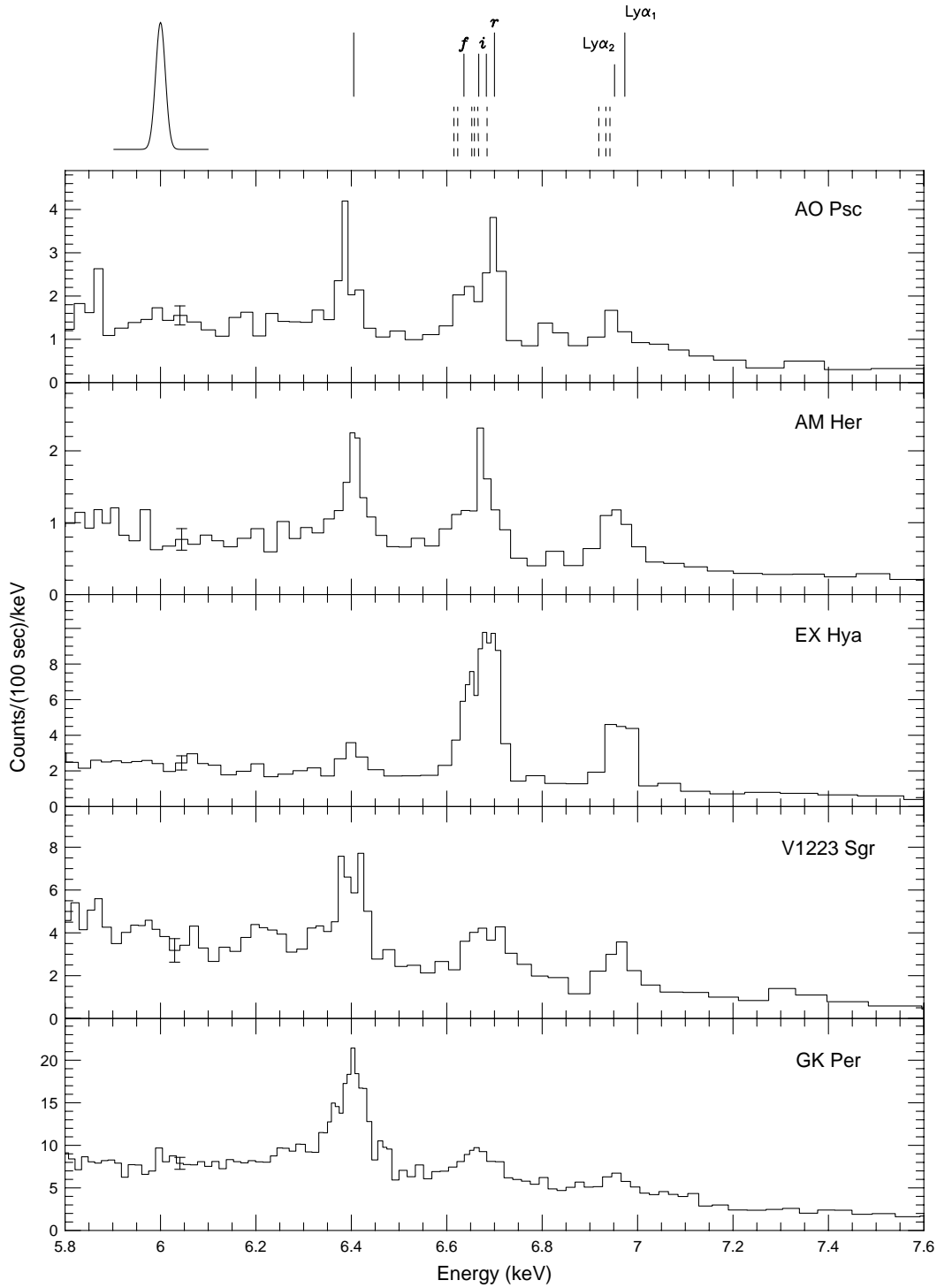


Figure 1. The iron $K\alpha$ region of *Chandra* HEG spectra of 5 MCVs. At top we show the locations of the $Ly\alpha_1$ and $Ly\alpha_2$ components of H-like iron; the resonance, intercombination and forbidden components of He-like iron; and the fluorescence line of cold iron. The dashed lines show the locations of major dielectronic satellite lines. The Gaussian illustrates the nominal resolution of the HEG at this energy. All spectra are binned to a minimum of 30 counts per bin (50 for GK Per), and thus have a typical signal-to-noise ratio (S/N) of 6 (8 for GK Per). A typical error bar is shown near 6 keV.

star (the MEG data are not useful at this energy and so are not shown here, but see Mukai et al. 2003).

The division into three distinct components is clear in all cases, conflicting with Hellier et al.'s (1998) report of blended lines, in particular in the *ASCA* SIS data of AO Psc. To investigate this further we show in Fig. 2 both the

Chandra HEG and the *ASCA* SIS spectra of AO Psc. The illustrative model is a power law and three Gaussians fitted to the *Chandra* data. The same model (adjusting only the power-law normalisation) is shown plotted on the *ASCA* data after folding through the *ASCA* response.

The *ASCA* spectrum has a group of 4 high points be-

Star	Date	Exp. (ks)	Equivalent widths (eV)		
			6.4-keV	6.7-keV	6.97-keV
AO Psc	2001/05/23	98	101	165	138
AM Her	2003/08/15	93	120	148	119
EX Hya	2000/05/18	59	35	322	130
V1223 Sgr	2000/04/30	51	108	67	87
GK Per	2002/03/27	32	260	117	80
	2002/04/09	34			

Table 1. The observations and measured equivalent widths.

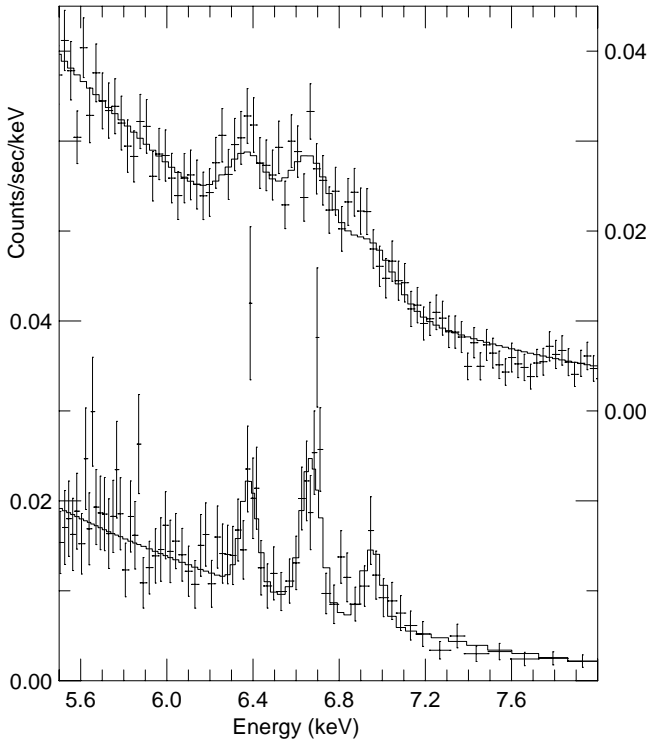


Figure 2. The iron $K\alpha$ region of AO Psc as observed with the ASCA SIS (top) and the *Chandra* HEG (bottom). The illustrative model is a power law and three Gaussians (at 6.38, 6.67 and 6.96 keV, all of width 35 eV). The fit parameters are optimised for the *Chandra* data alone.

tween the H-like and He-like lines, explaining why the ASCA spectrum is best fit by very broad, blended H-like and He-like lines. This is not supported by the higher-resolution *Chandra* data (though there are two high points in a similar place). Overall we suggest that apparent broadening in the ASCA spectrum is a statistical fluke, although a change in the source characteristics cannot be ruled out, and we await an *Astro-E2* spectrum to finally settle the issue.

It is also possible that the narrow lines seen in the *Chandra* data are accompanied by a broad, faint, Compton-scattered base that is hard to detect in high-resolution but low-S/N grating spectra. Indeed, this is expected to some degree (see Hellier et al. 1998), since the resonance lines are likely to be borderline optically thick, increasing the path length of resonance-line photons to the point where Comp-

ton scattering is appreciable (see also Terada et al. 2001 for the effect of resonance scattering on equivalent widths).

3 THE H-LIKE LINE

The ‘6.97-keV’ line of Fe XXVI consists of $\text{Ly}\alpha_1$ at 6.973 keV and, with theoretically half the intensity, $\text{Ly}\alpha_2$ at 6.952 keV [these are transitions to $1s(^2S_{1/2})$ from $2p(^2P_{3/2})$ and $2p(^2P_{1/2})$ respectively]. Dielectronic recombination leads to satellite lines at slightly lower energies in the range 6.91–6.95 keV (the energy shift arises from the presence of a ‘spectator’ electron in a higher- n level; strictly they are He-like lines, but occur near the H-like line since the second electron is not in the ground state and so doesn’t perturb the energy as much). Calculations of the positions and intensities of the satellite lines are given by Dubau et al. (1981) while observations of the H-like complex in the solar spectrum can be found in Pike et al. (1996).

We can thus ask whether the satellite lines are contributing to the MCV spectra. Although we can’t resolve them at the HEG resolution, their presence would shift the line centroid to the red. Thus we used XSPEC’s FAKEIT facility to find that narrow $\text{Ly}\alpha_1$ and $\text{Ly}\alpha_2$ components alone would, folded through the HEG response and fitted with a Gaussian, produce a line centroid of 6.964 keV with a width (σ) of 9 eV.

Fitting the observed 6.97-keV lines with a Gaussian produced a redder centroid. A fit to all 5 stars simultaneously found a centroid of 6.958 ± 0.003 keV, with 6.964 ruled out at 90 per cent confidence. The measured width, at 24 ± 6 eV, was significantly greater than 9 eV.

To interpret this we need to consider possible Doppler shifts, since the 6-eV shift is equivalent to 260 km s^{-1} and the broadening to 1000 km s^{-1} . We thus repeated the analysis on the H-like lines of Ne, Mg and Si, using the MEG data. Since the strength of satellite lines scales as z^4 , these lines should be free of satellites. We found no shifts to a 90-per-cent limit of 100 km s^{-1} and no broadening to a limit of 450 km s^{-1} . This doesn’t completely exclude Doppler shifts in the Fe lines, since the Fe emission centroid will be hotter and higher up the accretion column, where velocities are larger. However, the low level of any Doppler shifts suggests that the observed shift in H-like Fe is instead caused by the presence of satellite lines.

The lack of Doppler shifts to a limit of 100 km s^{-1} is somewhat surprising, considering that the escape velocity of a $0.7\text{-}M_{\odot}$ white dwarf is $\sim 5000 \text{ km s}^{-1}$. However, the in-fall velocity drops by a factor 4 through the stand-off shock, and reduces further as the material cools and settles onto the white dwarf (scaling with height as $h^{2/5}$; e.g., Frank, King & Raine 2002). Since the density scales inversely to the velocity, and since the X-ray emissivity depends on density squared, the emission is predominantly from low-velocity material close to the white dwarf surface. Further, the projection onto the line of sight, and the fact that the projected motions will be smeared out over the spin cycle, can reduce the observed velocities by another factor 2–3. Thus the observed 100-km s^{-1} limit is explained if the emission arises predominantly from the lowest few per cent of the accretion column.

4 THE HE-LIKE LINE

The ‘6.7-keV’ line of Fe XXV consists of the resonance line, *r*, a forbidden line, *f*, and two intercombination lines, *i* [being transitions to the ground state $1s^2(^1S_0)$ from $1s2p(^1P_1)$, $1s2s(^3S_1)$ and $1s2p(^3P_{2,1})$ respectively]. Interspersed with these are dielectronic satellite lines over the range 6.61–6.68 keV. The relative line intensities depend on temperature, density, the degree of photoionization, and the extent to which the resonance line is depleted by Compton scattering (which is greatly enhanced by resonant trapping of such photons). Calculations of the 6.7-keV complex can be found in Bautista & Kallman (2000) and Oelgoetz & Pradhan (2001). Such calculations indicate that satellite lines will dominate the 6.7-keV complex at temperatures below 3×10^7 K, with the He-triplet components dominating at higher temperatures.

At the *Chandra* resolution the different components are not resolved, but some tentative statements can be made. The AO Psc spectrum is compatible with a strong resonance component and contributions from the forbidden lines, or nearby satellites. The relative strength of the resonance line implies a temperature of $> 3 \times 10^7$ K [see the diagnostic curves in Bautista & Kallman (2000) and Oelgoetz & Pradhan (2001)].

In contrast, in the AM Her spectrum the resonance line appears weaker, with the intercombination lines, or adjacent satellites, appearing strongest. One possibility is that resonant scattering is affecting this line (a resulting beaming of resonance-line photons is already thought to be important in some AM Her stars; Terada et al. 2001).

Alternatively, a weak resonance line could result from a low temperature of $< 2 \times 10^7$ K (< 2 keV). At such temperatures the line will be dominated by satellite lines, assuming that collisional equilibrium holds. A low temperature is consistent with the lack of Doppler shifts, since $v/v_{\text{shock}} = T/T_{\text{shock}}$, so that the observed 100-km s $^{-1}$ limit implies a temperature in the line emitting region of $\lesssim 0.2 T_{\text{shock}}$. On the other hand, Ishida et al. (1997) deduce a temperature of 10–15 keV from the line ratios observed in the ASCA spectrum of AM Her, which is incompatible with our interpretation. Both of these temperature estimates are based on barely-resolved line data, so we await *Astro-E2* for more reliable results.

A possible explanation for AM Her being different from AO Psc is that AM Her, being a polar, has a much stronger magnetic field of 14 MG (Bailey, Ferrario & Wickramasinghe 1991), whereas the other stars have weaker fields of ~ 1 MG. Thus cyclotron cooling will be important in AM Her, but not in the others.

The EX Hya data suggest a strong resonance line, along with *i*, and *f* and/or satellites. Overall, the ratio of He-like/H-like equivalent widths is very different from that in the other systems (Table 1). Similarly, Mukai et al. (2003) found that the EX Hya spectrum is unlike that of other magnetic MCVs, being compatible with a collisionally-excited, cooling-flow model, whereas others showed photoionized spectra. The difference is probably due to the much lower accretion rate and luminosity of EX Hya, which are in line with it being the only system in our sample below the period gap.

5 THE FLUORESCENCE LINE

The fluorescence line peaks near 6.41 keV in all stars, compatible with cold iron in states Fe I to Fe XVII. There is little sign of iron at ionizations between XVII and XXV.

The GK Per fluorescent line has the highest S/N. It has a red wing extending to 6.33 keV, consistent with a Doppler shift of up to 3700 km s $^{-1}$. We suggest that this arises from pre-shock material, which will be falling at near the white-dwarf escape velocity.

Further, the GK Per line appears to have a fainter shoulder to its red wing, extending to 170 eV from the line centre. We suggest that these are photons Compton downscattered by up to two Compton wavelengths.

It is notable that GK Per’s fluorescent line has an equivalent width more than a factor two greater than seen in the other systems (Table 1). Since this line arises from scattering of the emitted X-rays, the equivalent width will be set primarily by the size of the scattering targets, namely the white dwarf (filling half the solid angle as seen from the emission region) and the inflowing material.

In most MCVs material accretes only over a small range of magnetic longitude, as deduced from eclipse studies of the size of the emission region (e.g. Hellier 1997), and from the blackbody areas of regions of heated white-dwarf surface (e.g. Haberl & Motch 1995). Thus the ‘accretion curtains’ of infalling material are a small target compared to the white dwarf, in keeping with the fact that the fluorescent lines are not Doppler-shifted wholesale.

However, from an analysis of the spin-cycle pulsation of GK Per, Hellier, Harmer & Beardmore (2004) claimed that, during outburst, the material accretes from all azimuths to form a complete accretion ring. This would fill most of the sky, as seen from the emission region, thus greatly enhancing the equivalent width of the fluorescent line. In keeping with this idea the fluorescent line observed in quiescence by ASCA is much weaker, with an equivalent width of only 50 eV (Hellier et al. 1998).

6 CONCLUSIONS

We present the first compilation of Fe K α -line spectra of MCVs using the *Chandra*-HETG. We conclude that:

(1) Dielectronic satellite lines are detected in the H-like and He-like iron K α lines. These cause the lines to be broadened and redshifted, as predicted by Oelgoetz & Pradhan (2001).

(2) The H-like lines show no Doppler shifts to a limit of 100 km s $^{-1}$. This implies that the emission is predominantly from the lowest few per cent of the accretion columns, where the density is highest.

(3) The H-like and He-like lines of AO Psc are not Compton broadened by 150 eV, as had been suggested from a lower-resolution ASCA spectrum.

(4) The He-like lines in AO Psc and AM Her show a discernably different structure. This could be caused by greater cyclotron cooling in AM Her.

(5) The absence of Doppler shifts and the hints of structure in the He-like line are encouraging for observations with the XRS on the forthcoming *Astro-E2*. Its 6-eV resolution will separate the different He-triplet and satellite lines, allowing the application of temperature diagnostics.

(6) The fluorescence line in GK Per shows a Doppler-shifted red wing owing to pre-shock material falling at near the escape velocity. We also detect a fainter, 170-eV shoulder caused by Compton down-scattering. The high equivalent width of GK Per's fluorescence line supports the suggestion by Hellier et al. (2004) that, during outburst, the accretion flows from all azimuths to form a complete accretion ring.

REFERENCES

- Aizu K., 1973, *Prog. Theor. Phys.*, 49, 1184
 Bailey J., Ferrario L., Wickramasinghe D. T., 1991, *MNRAS*, 251, P37
 Bautista M. A., Kallman T. R., 2000, *ApJ*, 544, 581
 Cropper M., Wu K., Ramsay G., Kocabiyyik A., 1999, *MNRAS*, 306, 684
 Dubau J., Loulergue M., Gabriel A. H., Steenman-Clark L., Volonte S., 1981, *MNRAS*, 195, 705
 Frank J., King A., Raine D. J., 2002, *Accretion Power in Astrophysics*. Cambridge Univ. Press, Cambridge
 Fujimoto R., Ishida M., 1997, *ApJ*, 474, 774
 Haberl F., Motch C., 1995, *A&A*, 297, L37
 Hellier C., 1997, *MNRAS*, 291, 71
 Hellier C., Harmer S., Beardmore A. P., 2004, *MNRAS*, 349, 710
 Hellier C., Mukai K., Osborne J. P., 1998, *MNRAS*, 297, 526
 Ishida M., Matsuzaki K., Fujimoto R., Mukai K., Osborne J. P., 1997, *MNRAS*, 287, 651
 Mauche C. W., Liedahl D. A., Fournier K. B., 2001, *ApJ*, 560, 992
 Mauche C. W., Liedahl D. A., Fournier K. B., 2003, *ApJ*, 588, L101
 Mukai K., Kinkhabwala A., Peterson J. R., Kahn S. M., Paerels F., 2003, *ApJ*, 586, L77
 Norton A. J., Watson M. G., King A. R., 1991, in Treves A., Perola G., Stella L., eds, *Lecture Notes in Physics Vol. 385, Iron Line Diagnostics in X-ray Sources*, Springer-Verlag, Heidelberg, p. 155.
 Oelgoetz J., Pradhan A. K., 2001, *MNRAS*, 327, L42
 Pike C. D. et al. 1996, *ApJ*, 464, 487
 Terada Y., Ishida M., Makishima K., Imanari T., Fujimoto R., Matsuzaki K., Kaneda H., 2001, *MNRAS*, 328, 112